



# Trends in Effective Diffusion Coefficients for Ion-Exchange Strengthening of Soda-Lime-Silicate Glasses

Stefan Karlsson<sup>1,2\*</sup>, Lothar Wondraczek<sup>2</sup>, Sharafat Ali<sup>3,4</sup> and Bo Jonson<sup>3</sup>

<sup>1</sup>RISE Research Institutes of Sweden, RISE Glass section, Växjö, Sweden, <sup>2</sup>Otto Schott Institute of Materials Research, Friedrich Schiller University of Jena, Jena, Germany, <sup>3</sup>Faculty of Technology – Glass Group, Linnaeus University, Växjö, Sweden, <sup>4</sup>Science and Technology Division, Corning Incorporated, Corning, NY, USA

Monovalent cations enable efficient ion-exchange processes due to their high mobility in silicate glasses. Numerous properties can be modified in this way, e.g., mechanical, optical, electrical, or chemical performance. In particular, alkali cation exchange has received significant attention, primarily with respect to introducing compressive stress into the surface region of a glass, which increases mechanical durability. However, most of the present applications rely on specifically tailored matrix compositions in which the cation mobility is enhanced. This largely excludes the major area of soda-lime-silicates (SLS) such as are commodity in almost all large-scale applications of glasses. Basic understanding of the relations between structural parameters and the effective diffusion coefficients may help to improve ion-exchanged SLS glass products, on the one hand in terms of obtainable strength and on the other in terms of cost. In the present paper, we discuss the trends in the effective diffusion coefficients when exchanging Na<sup>+</sup> for various monovalent cations (K<sup>+</sup>, Cu<sup>+</sup>, Ag<sup>+</sup>, Rb<sup>+</sup>, and Cs<sup>+</sup>) by drawing relations to physicochemical properties. Correlations of effective diffusion coefficients were found for the bond dissociation energy and the electronic cation polarizability, indicating that localization and rupture of bonds are of importance for the ion-exchange rate.

**Keywords:** ion exchange in glass, float glass, soda-lime-silicate, effective diffusion coefficients, bond dissociation energy, electronic cation polarizability

## INTRODUCTION

Monovalent cations exhibit pronounced mobility in silicate glasses. This enables highly effective ion-exchange processes. In this context, ion exchange has long been known as a useful tool to modify the surface of glass products (Schulze, 1913; Stern, 1966). Numerous properties can be modified in this way, including mechanical, optical, electrical, and chemical performance. In particular, alkali cation exchange has received significant attention throughout the years, primarily with respect to introducing compressive stresses into the surface layer, which increases mechanical durability (Gy, 2003; Karlsson et al., 2010a; Varshneya, 2010a,b). This specific subject has been developing into a large market, where ion exchange strengthened glasses are now used in displays, handheld electronic devices, pharmaceutical packaging, and many other areas. Monovalent cation exchange has also received much attention for tailoring the refractive index profile of the surface layer, i.e., so as to create microstructured planar or buried waveguides or optical lenses with graded refractive

## OPEN ACCESS

### Edited by:

Sylwester Janusz Rzoska,  
Polish Academy of Sciences, Poland

### Reviewed by:

Roger Jay Loucks,  
Alfred University, USA  
Jean-Marc Delaye,  
CEA, France

### \*Correspondence:

Stefan Karlsson  
stefan.karlsson@ri.se

### Specialty section:

This article was submitted  
to Glass Science,  
a section of the journal  
Frontiers in Materials

**Received:** 10 February 2017

**Accepted:** 31 March 2017

**Published:** 24 April 2017

### Citation:

Karlsson S, Wondraczek L, Ali S and  
Jonson B (2017) Trends in Effective  
Diffusion Coefficients for Ion-  
Exchange Strengthening of  
Soda-Lime-Silicate Glasses.  
*Front. Mater.* 4:13.  
doi: 10.3389/fmats.2017.00013

index (Ramaswamy and Srivastava, 1988; Opilski et al., 2000; Honkanen et al., 2006; Tervonen et al., 2011).

The ion-exchange process can be described as an interdiffusion reaction where the rate of reaction is described by Fick's laws of diffusion (Nordberg et al., 1964). While usually, the concentration gradient ( $\partial c/\partial x$ ) is considered, the actual driving force for ionic transport is the gradient in chemical potential ( $\partial\mu/\partial x$ ) between the different ionic media (Schaeffer, 2012) (which in many cases, correlates linearly with the gradient in chemical composition). The transport coefficient is usually concentration-dependent (Doremus, 1964),

$$\bar{D} = \frac{D_1 D_2}{N_1 D_1 + N_2 D_2}, \quad (1)$$

where in a simplistic approximation,  $D_1$  and  $D_2$  are the coefficients of self-diffusion of contributing species 1 and 2,  $N_1$  and  $N_2$  are the corresponding relative atomic fractions, and  $\bar{D}$  is the effective diffusion coefficient.

In the present understanding of ion-exchange kinetics, the transport coefficient is governed by many different parameters, such as salt-bath composition (the diffusion reservoir), glass composition (the structure and free volume of the matrix), exchanging ion species (size and charge), temperature, pressure, etc. The glass composition has received much attention over the years and the specific components of alumina (Burggraaf, 1966), phosphate (Bartholomew and Garfinkel, 1980), and zirconia (Nordberg et al., 1964) have been shown to have beneficial effects on chemical strengthening through acting on free volume, oxygen packing density, and degree of cross-linking of the structural backbone. Transport properties and the relation to glass composition are mostly understood on the basis of conductivity/diffusion paths across which the considered ions are transported, as originally proposed by Greaves (1985). The presence of such paths was later indicated by, e.g., AFM analyses by Frischat et al. (2004), see **Figure 1**. For each alkali charge that is added to the

glass composition, one non-bridging oxygen (NBO) is created so that the network is depolymerized. The NBOs are negatively charged and are charge-compensated by the positively charged alkali ions. This is what leads to the postulated creation the mentioned paths of mobility. There are various models that aim to describe transport properties in glasses, including the strong electrolyte approach (Anderson and Stuart, 1954) or the weak electrolyte approach (Ravaine and Souquet, 1977). Despite their disadvantages (Martin and Angell, 1986), these models provide a decent understanding that by changing the glass composition (e.g., through introduction of  $\text{Al}_2\text{O}_3$ ,  $\text{B}_2\text{O}_3$ , and/or  $\text{P}_2\text{O}_5$ ), the number of NBOs is varied. This is discussed by Grandjean et al. (2007) and Smedskjaer et al. (2011) where the latter suggests that the alkali ions diffuse faster when acting as charge compensators to, e.g.,  $\text{Al}^{3+}$  or  $\text{B}^{3+}$ , as opposed to acting as a creator of NBO. The model then rationalizes attractive reactions among cation species and their effect on the overall activation energy. Major additional factors which then affect the transport properties (Bunde et al., 1996) include site mismatch, site relaxation (frequently called structural relaxation), interionic interaction, and the mixed-modifier effect (Maass et al., 1992; Karlsson et al., 2015; Poletto Rodrigues et al., 2016; Griebenow et al., 2017).

Industrially, the ion-exchange strengthening process is typically performed on rolled or drawn sheet glass by immersing the glass for a prolonged time into appropriate salt melts (Karlsson et al., 2010a). Employed glass compositions are typically chosen for high ion mobility and high conversion to compressive stress, e.g., alkali-aluminosilicates (Burggraaf and Cornelissen, 1964; Burggraaf, 1966; Ragoen et al., 2017), aluminoborosilicates (Morozumi et al., 2015), and, more recently, aluminophosphosilicates (Zeng et al., 2016). The salt composition is then selected from a trade-off between desired exchange species, high treatment temperature, low vapor pressure, target depth of layer and surface stress, and cost. In the present paper, we discuss trends in the effective diffusion coefficients when exchanging  $\text{Na}^+$  for various monovalent cations ( $\text{K}^+$ ,  $\text{Cu}^+$ ,  $\text{Ag}^+$ ,  $\text{Rb}^+$ , and  $\text{Cs}^+$ ) in the surface

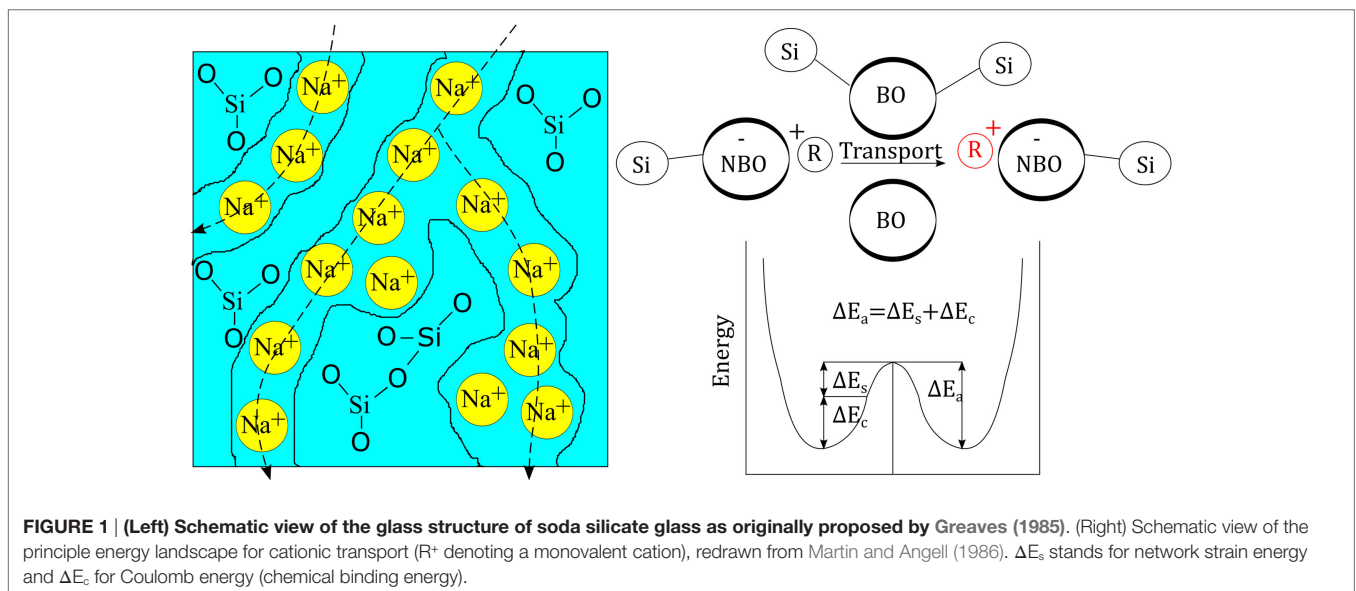


**FIGURE 1 | (Left) Schematic view of the glass structure of soda silicate glass as originally proposed by Greaves (1985). (Right) Schematic view of the principle energy landscape for cationic transport ( $\text{R}^+$  denoting a monovalent cation), redrawn from Martin and Angell (1986).  $\Delta E_s$  stands for network strain energy and  $\Delta E_c$  for Coulomb energy (chemical binding energy).**

of soda-lime-silicate (SLS) float glass. Knowing more about what affects the effective diffusion coefficients can potentially help to improve the diffusivity in chemically strengthened glasses or planar waveguides. For this, we reconsider previously published data (Karlsson et al., 2010b, 2012, 2013).

## MATERIALS AND METHODS

Data used in this report are collected from studies which have previously been published by us (Karlsson et al., 2010b, 2012, 2013). For clarification, we provide a summarized overview of the experimental procedures. In all studies, the employed glass was a commercial SLS float glass (Pilkington Floatglas AB, Halmstad, Sweden), see the nominal composition in **Table 1**.

Other than in the regular immersion technique, for ion exchange, a different approach was used where the salt mixture was applied directly onto the float glass surface as a solid paste before melting and heat treatment. Experimental information on the salts and thermal treatments are summarized in **Table 2**. Salts were applied on the air-side of the glass and the ion exchange itself was performed over a time of 10 h, following the heating procedure to the target temperature, which took 1 h. Subsequent cooling was done at approximate rates of 2 K/min.

The resulting surface concentration profiles were measured by different techniques, UV-VIS spectrophotometry, atomic absorption spectroscopy (AAS), and energy dispersive spectroscopy in Scanning Electron Microscopy. Wet-chemical surface ablation (SAC) was employed before chemical analysis using UV-VIS and AAS. The surface ablation cell (SAC) technique was developed and tested in a round-robin project of Technical Committee 2 of the International Commission on Glass as an efficient tool for multielement determination of glass surface chemistry with scalable matrix dependence, see **Figure 2** (Sundberg et al., 2010). More details on the handling of the SAC and analytical procedures can be found in previous reports (Karlsson et al., 2010b, 2012; Sundberg et al., 2010; Karlsson, 2012). In this way, depth-resolved concentration data were obtained for the various species in the glass.

The effective diffusion coefficient  $\bar{D}$  (cm<sup>2</sup>/s) was then calculated using Eq. 2, frequently called Green's function, but really

**TABLE 1 | Nominal chemical composition of the investigated float glass.**

Oxides	SiO <sub>2</sub>	Na <sub>2</sub> O	CaO	MgO	SO <sub>3</sub>	Al <sub>2</sub> O <sub>3</sub>	Fe <sub>2</sub> O <sub>3</sub>	K <sub>2</sub> O	TiO <sub>2</sub>
wt%	72.5	13.7	9.12	4.14	0.247	0.13	0.103	0.04	0.01
mol%	71.0	13.0	9.57	6.05	0.182	0.08	0.038	0.03	0.01

**TABLE 2 | Ion-exchange treatments.**

Ion	Salt	Salt mixture	Mass of salt(s) (g)	H <sub>2</sub> O (g)	Temperatures °C
K <sup>+</sup>	KNO <sub>3</sub> :KCl	I: 2:1 (wt ratio)	6	1.5	460, 480, 500, 520
K <sup>+</sup>	KNO <sub>3</sub> :KCl	II: 1:2 (wt ratio)	6	1.5	460, 480, 500, 520
Cu <sup>+</sup>	CuCl	–	6	2	460, 480, 500, 520
Ag <sup>+</sup>	AgCl	–	5	2	460, 470, 480, 500, 520
Rb <sup>+</sup>	RbCl:NaCl	53.75:46.25 mol%	6	1	530, 540
Cs <sup>+</sup>	CsCl:NaCl	65:35 mol%	6	1	520, 530

a fundamental solution of Fick's second law for a semi-infinite planar situation with finite diffusion reservoir, a starting surface concentration of 100% in an infinitely thin surface layer, and a starting matrix concentration of zero (Karlsson et al., 2010b).

$$C = \frac{A}{\sqrt{t}} e^{-x^2/4\bar{D}t}, \quad (2)$$

The analyzed concentration ( $C$ ) and the calculated depth ( $x$ ) were plotted by  $\ln(C)$  vs.  $x^2$ , yielding the slope  $k = (-4\bar{D}t)^{-1}$ . This calculation is based on the mathematical assumption that the effective diffusion coefficient is independent of the concentration of diffusing ions and also independent of time. It is further mathematically assumed that the effective diffusion coefficient in the salt is equal to the effective diffusion coefficient in the glass, see **Figure 3** (Crank, 1975; Karlsson et al., 2010b).

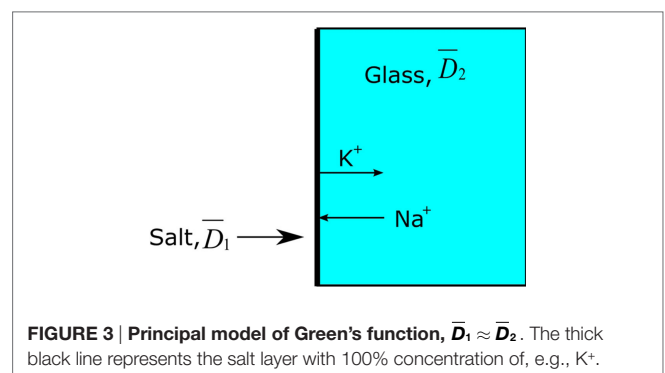
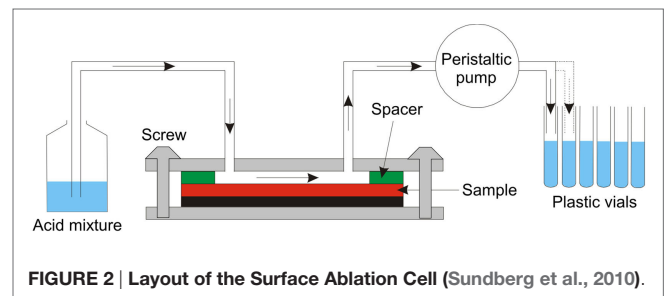
Calculations of the activation energy,  $E_a$  (kJ/mol), for ionic interdiffusion were made by use of the Arrhenius equation, Eq. 3. Plotting  $\ln \bar{D}$  vs.  $T^{-1}$  gives the slope  $k = -E_a/R$  and the intercept  $m = \ln D_0$ . This assumes that the activation energy is independent of temperature (Frischat, 1975).

$$\bar{D} = D_0 e^{\left(\frac{-E_a}{RT}\right)}, \quad (3)$$

The cation field strength (CFS) is calculated through Eq. 4 (Vogel, 1994), where the  $z$  is the charge of the cation and  $r$  is the effective ionic radius in ångström of the cation and anion as given by Dietzel (1942). The ionic radii data were taken from Shannon (1976).

$$CFS = \frac{z_{cat}}{(r_{cat} + r_{an})^2} \quad (4)$$

The electronic cation polarizability ( $\alpha$ ) was calculated using the Lorentz-Lorenz relation (Eq. 5), and values of molar refractivity



(A) as calculated by Pauling (1927).  $N$  denotes the amount of polarizable ions normally assumed to be equal to Avogadro's number ( $N_A$ ).

$$A = \frac{4\pi}{3} N\alpha \quad (5)$$

## TRENDS IN EFFECTIVE DIFFUSION COEFFICIENTS

The employed approach provides a simplistic approximation of the practical diffusion rate, expressed through the effective diffusion coefficient according to the Green's function. It has been shown before that the obtained values are in reasonable agreement with other published data (Pask and Parmelee, 1943; Shaisha and Cooper, 1981; Gonella et al., 1998; Liu and Pun, 2004; Karlsson et al., 2010b, 2012). In a practical consideration, the effective diffusion coefficient represents the efficiency of the ion-exchange reaction, in other words, the rate of the ion exchange. The effective diffusion coefficients are calculated from the concentration vs. depth profile data. In the present case, the penetration depths of  $K^+$  for the two salt mixtures on the air-side of float glass are exceeding or equal to 25–30  $\mu\text{m}$  for all temperatures after 10 h of ion exchange (Karlsson et al., 2010b). The penetration depth is approximately 8–10  $\mu\text{m}$  for  $Rb^+$  (Karlsson et al., 2012). In the periodic table, Rb is the next element in the group after potassium. Despite the considerably larger ionic radius, it is possible to perform ion exchange thermally with  $Rb^+$ .  $Cs^+$  has an even larger ionic radius than  $Rb^+$ , but still, also  $Cs^+$ - $Na^+$  ion exchange is possible. The corresponding penetration depth of  $Cs^+$  was found at approximately 5–7  $\mu\text{m}$ . Compared to  $Rb^+$ - $Na^+$  ion exchange, much smaller concentrations of  $Cs_2O$  were found in the surface layers (Karlsson et al., 2012). The determined concentration vs. depth profiles of copper ion exchange revealed that the total copper concentration, expressed as mol% [Cu], is relatively high at the top surface layers, but decreases substantially in the top  $\sim 5$   $\mu\text{m}$  of the samples. Deeper in the sample, the slope of the concentration profile appears to change, indicating a change in the underlying transport mechanism. According to our previous interpretation (Karlsson et al., 2012), the shape of the diffusion profile suggests that for a depth of  $>5$   $\mu\text{m}$ , copper diffusion is unaffected by variations of the chemical composition. From it is indicated that in the range of 0 to  $\sim 5$   $\mu\text{m}$ , the profile is controlled by sodium outward-diffusion and whereas beyond  $\sim 5$   $\mu\text{m}$ , it is controlled by the movement of  $Cu^+$  species. The reason for this is that  $Na^+$  will eventually be depleted at the top surface whereas the opposite is the case for the interior (Karlsson et al., 2012). The copper ion exchanged air-sides were transparent and uncolored after the treatment. This indicates that no substantial amounts of  $Cu^{2+}$  or nanoparticles ( $Cu^0$  or  $Cu_2O$ ) were formed and that most of the copper is incorporated as  $Cu^+$  ions in the glass (Karlsson et al., 2012) as compared to treatments on the tin-side (Karlsson et al., 2013). The diffusion of  $Ag^+$  in glass is known to be relatively high, confirmed by the data in Table 3. The penetration depth of  $Ag^+$  ion exchange ranges from 80–100  $\mu\text{m}$  for samples treated at 460°C to 150–200  $\mu\text{m}$  for samples treated at 520°C. The  $Ag^+$ - $Na^+$  ion exchanged samples were colored yellowish after treatment.

The corresponding profiles and discussions of ion exchange with noble metal ions can be found in Karlsson et al. (2010b, 2012). All effective diffusion coefficients from our previous work are summarized in Table 3. Note that these data are in good agreement with the data published by others, thus the below described trends should be regarded as general observations.

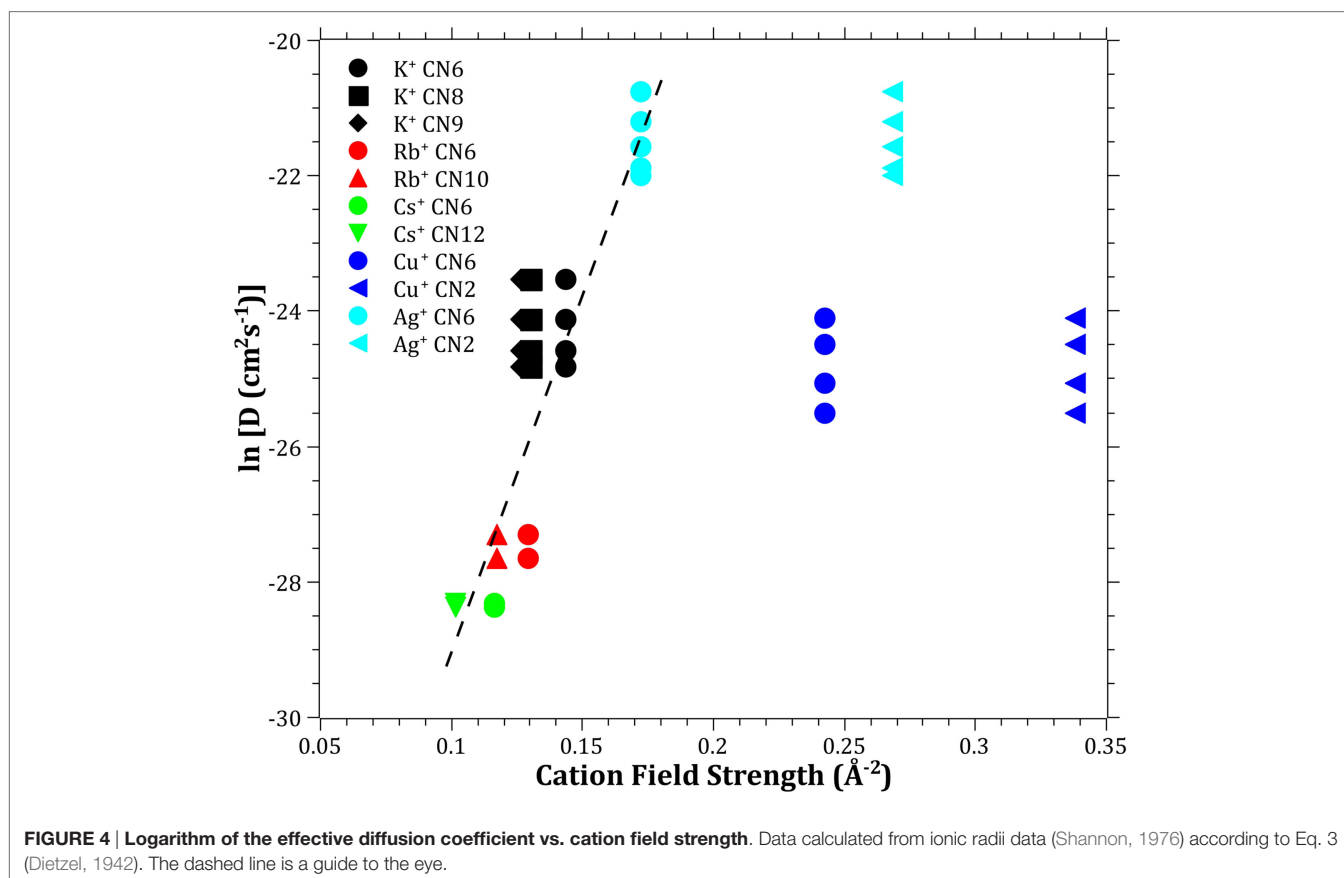
The diffusivities of the studied monovalent cations follow the order  $Ag^+ > K^+ > Cu^+ > Rb^+ > Cs^+$ . This is in accordance with the order of ionic radii for the alkali ions ( $K^+ < Rb^+ < Cs^+$ ). However, an opposite pattern is found for the noble metal ions, where the ionic radii  $Cu^+ < Ag^+$ . This trend is evident in Figure 4, where  $\ln \bar{D}$  is plotted vs. CFS. A similar trend is seen when plotting  $\ln \bar{D}$  vs. ionic radii as the value of CFS is physically equivalent to the ionic radius when charge and anion species are of equivalent ionic radius. Several different values of the ionic radii were used for calculating CFS, depending on the coordination numbers (CN), see Table 4. When assuming CN6,  $K^+$ ,  $Rb^+$ ,  $Cs^+$ , and  $Ag^+$  seem to follow a relatively linear relationship. However, for the commonly assumed CN2 of noble metal ions in silicate glass, this trend cannot be seen. CN for  $Cu^+$  are given in Kamiya et al. (1992), d'Acapito et al. (1997), Lee et al. (2000), Gonella et al. (2005), Arletti et al. (2006), Farges et al. (2006), Gliozzo et al. (2010), and Klysubun et al. (2011) and for  $Ag^+$  in Houde-Walter et al. (1993), Dubiel et al. (1997), Yang et al. (2003), and Yang and Dubiel (2007).

The coordination environment of different cations is complex.  $Na^+$  cations have been reported with a mean CN in the range of 4–6 (Greaves, 1981; Greaves et al., 1981; Vessal et al., 1992; Houde-Walter et al., 1993; Cormack and Du, 2001; Du and Cormack, 2004; Bernasconi et al., 2012; Kreski et al., 2012) in silicate glass, but also lower (Dubiel et al., 1997) or higher (McKeown et al., 1985; George and Stebbins, 1996; Weigel et al., 2008) values have been mentioned, depending on compositional changes.  $K^+$  cations have been reported to most likely have a CN of 8–10 (Jackson et al., 1987; Cormier et al., 2010; Kreski et al., 2012), but here as well, 4–6 have also been reported (Greaves et al., 1991; Kamijo et al., 1996), again depending on composition.  $Rb^+$  (Vessal et al., 1992) and  $Cs^+$  (Greaves et al., 1991) cations have been reported to have a CN of 5–6, apart from the study of Stefanovsky and Purans (2012) in nuclear waste glasses where  $Cs^+$  was found to have CNs of 6–12. Finally, similar versatility is found in literature for  $Li^+$ , with CN of 3–4 (Uhlir et al., 1996; Zhao et al., 1998) and 3–6 (Xu and Stebbins, 1995). As can be seen in Table 4, the effects of the CN differences for the alkalis are not as strong as for the noble metal ions.

The Pauling electronegativity of the elements vs.  $\ln \bar{D}$  does not give the same trend ( $Ag^+$  fitting-in with the alkali metal ions) as was the case for ionic radii and CFS, see Figure 5. It also does not give any further insight as to why  $Ag^+$  is faster diffusing than  $Cu^+$ . The noble metal cations have considerably higher ionization energies than the alkalis and, thereby, higher electronegativity. Tabulated electronegativity values do not provide a reasonable answer to this, and one reason can be that the electronegativity may also change depending on the environment of the cation. The enthalpy of formation,  $\Delta H_f$ , of the oxides, gives a decreasing exponential trend for the alkali down in the group and it does not fit with neither  $Cu_2O$  nor  $Ag_2O$ , see Figure 6. The Gibbs free energy of formation gives a similar trend as enthalpy of formation,

**TABLE 3 | Overview of effective diffusion coefficients ( $\text{cm}^2\text{s}^{-1}$ ) of several monovalent cations in commercial float glass during 10 h of ion exchange (Karlsson et al., 2010b, 2012, 2013).**

Temperatures °C	Ag <sup>+</sup>	K <sup>+(I)</sup>	K <sup>+(II)</sup>	Cu <sup>+</sup>	Rb <sup>+</sup>	Cs <sup>+</sup>
540	–	–	–	–	$1.4 (\pm 0.1) 10^{-12}$	–
530	–	–	–	–	$9.8 (\pm 0.5) 10^{-13}$	$5.0 (\pm 0.3) 10^{-13}$
520	$9.6 (\pm 1.0) 10^{-10}$	$6.1 (\pm 0.3) 10^{-11}$	$6.0 (\pm 0.3) 10^{-11}$	$3.4 (\pm 0.2) 10^{-11}$	–	$4.8 (\pm 0.2) 10^{-13}$
500	$6.2 (\pm 0.6) 10^{-10}$	$3.2 (\pm 0.2) 10^{-11}$	$3.5 (\pm 0.2) 10^{-11}$	$2.3 (\pm 0.1) 10^{-11}$	–	–
480	$4.3 (\pm 0.4) 10^{-10a}$	$2.1 (\pm 0.1) 10^{-11}$	$2.1 (\pm 0.1) 10^{-11}$	$1.3 (\pm 0.1) 10^{-11}$	–	–
470	$3.1 (\pm 0.3) 10^{-10a}$	–	–	–	–	–
460	$2.8 (\pm 0.3) 10^{-10}$	$1.5 (\pm 0.1) 10^{-11}$	$1.8 (\pm 0.1) 10^{-11}$	$8.4 (\pm 0.4) 10^{-12}$	–	–
Activation energy, $E_a$ (kJ/mol)	105 ( $\pm 21$ )	111 ( $\pm 11$ )	100 ( $\pm 10$ )	115 ( $\pm 12$ )	–	–
Penetration depth at lowest temperature ( $\mu\text{m}$ )	80–100	25–30	25–30	20–25	8–10	5–7

(I), salt mixture  $\text{KNO}_3:\text{KCl}2:1$ ; (II), salt mixture  $\text{KNO}_3:\text{KCl}1:2$ .<sup>a</sup>Calculated as an average of a double sample.

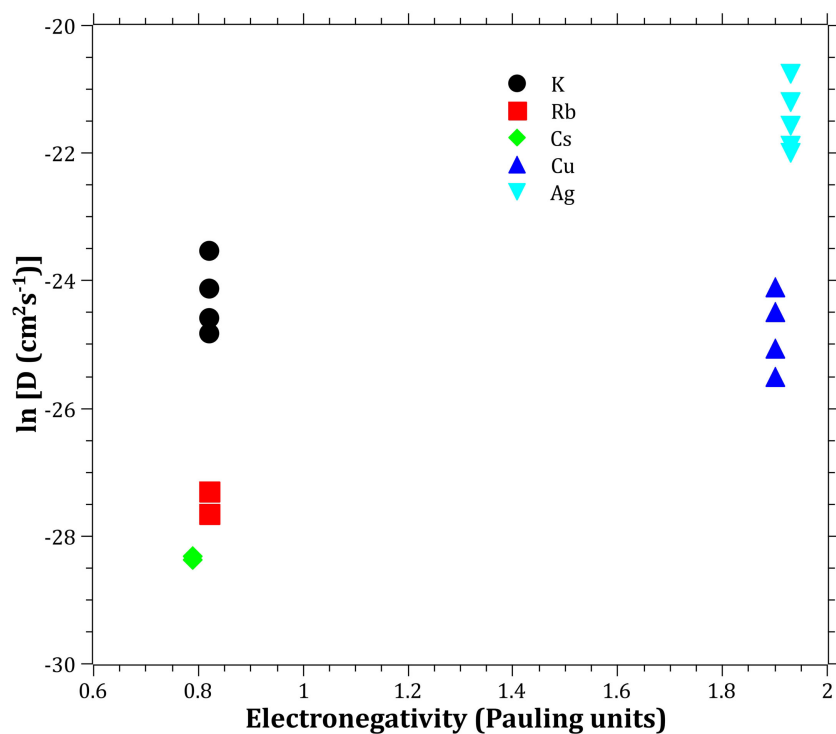
which is perfectly reasonable as it includes the enthalpy of formation. The dissociation energy of the bond to oxygen, on the other hand (Figure 7), gives a rather linear relationship between the alkali species and Ag-O. Cu-O has a considerably higher bond dissociation energy than the others, which perhaps offers the best explanation as to why Cu<sup>+</sup> is diffusing slower than Ag<sup>+</sup>. The bond dissociation energy includes all oxide bonds in the cation coordination sphere, in contrast to single bond strengths that can be estimated from the bond dissociation energy divided by the coordination number (Varshneya, 2006). It shall be noted that the bond dissociation energy shows a minimum for K<sup>+</sup> in the alkali series, see Table 3, indicating that K<sup>+</sup> is efficient for ion-exchange strengthening. The electronic ionic polarizability is a measure of

the effect that surrounding atoms in the vitreous network has on the dipole moment or orbital structure of the mobile species that we are considering. It is not just important for the optical properties (Karlsson et al., 2016) but also important for transport properties as electric fields are constantly changing as the ions diffuse in the glass (Frischat, 1975). The logarithm of the effective diffusion coefficient as a function of the electronic ionic polarizability is given in Figure 8, where Cu<sup>+</sup> fits into the trend with the alkali ions, while Ag<sup>+</sup> with relatively high polarizability has an unusually high effective diffusion. High electronic ionic polarizability can be argued to be a positive property on the activation energy of the diffusion as the ions are deformable during the diffusion, a concept that is considered when choosing materials as solid electrolytes

**TABLE 4 |** Data collected for understanding trends in the effective diffusion coefficients, following a representation in Vogel (1994).

Element	Ionic radius (Å) (Shannon, 1976)	Coordination numbers	Cation field strength (Å <sup>-2</sup> )	Electronegativity (Pauling units)	Enthalpy of formation (800 K), ΔH <sub>f</sub> (kJ/mol)	Bond dissociation energy per MO <sub>x</sub> (kJ/mol)	Estimated single bond strength (kJ/mol)	Electronic ionic polarizability (Å <sup>3</sup> ) (Pauling, 1927)	Aqueous ionic conductivity (S cm <sup>2</sup> /mol)
Li	0.59	4	0.292	0.98	-597.6	341 ± 6	85.3	0.029	38.69
Li	0.76	6	0.245	do	do	do	56.8	do	do
Li	0.92	8	0.210	do	do	do	42.6	do	do
Na	0.99	4	0.198	0.93	-414.2	257 ± 15	64.3	0.181	50.11
Na	1.02	6	0.192	do	do	do	42.8	do	do
Na	1.18	8	0.168	do	do	do	32.1	do	do
K	1.38	6	0.13	0.82	-367.4	239 ± 34	39.8	0.840	73.5
K	1.51	8	0.143	do	do	do	29.9	do	do
K	1.55	9	0.130	do	do	do	26.6	do	do
Rb	1.52	6	0.127	0.82	-315.9	255 ± 84	42.5	1.415	77.8
Rb	1.66	10	0.129	do	do	do	25.5	do	do
Cs	1.67	6	0.117	0.79	-301.2	297 ± 25	49.5	2.438	77.3
Cs	1.88	12	0.116	do	do	do	24.75	do	do
Cu	0.77	6	0.101	1.9	-165.3	343 ± 63	57.2	0.428	56.6 (Cu <sup>2+</sup> )
Cu	0.46	2	0.243	do	do	do	171.5	do	do
Ag	1.15	6	0.338	1.93	-26.4	213 ± 84	35.5	1.717	61.9
Ag	0.67	2	0.172	do	do	do	106.5	do	do

Data are taken from Dean (1999) unless otherwise stated.

**FIGURE 5 |** Logarithm of the effective diffusion coefficient vs. electronegativity. Data taken from Dean (1999).

(Cao et al., 2014). As for comparison, the ionic conductivity in aqueous solution as a function of the logarithmic effective diffusion coefficient also gives a similar trend as for the bond dissociation energy (Figure 9). While data for Cu<sup>+</sup> was not found in literature, the other species clearly follow the order Ag<sup>+</sup> > K<sup>+</sup> > Rb<sup>+</sup> > Cs<sup>+</sup>. The simple reason for the lack of data on Cu<sup>+</sup> is probably that it is difficult to stabilize Cu<sup>+</sup> in aqueous solutions.

## DISCUSSION

To understand and ultimately design glasses with increased mobility for chemically strengthening of glass, it is likely important to learn from the experiences in the field of solid electrolytes (Cao et al., 2014). The structural properties are of much importance, hence the following criteria should be

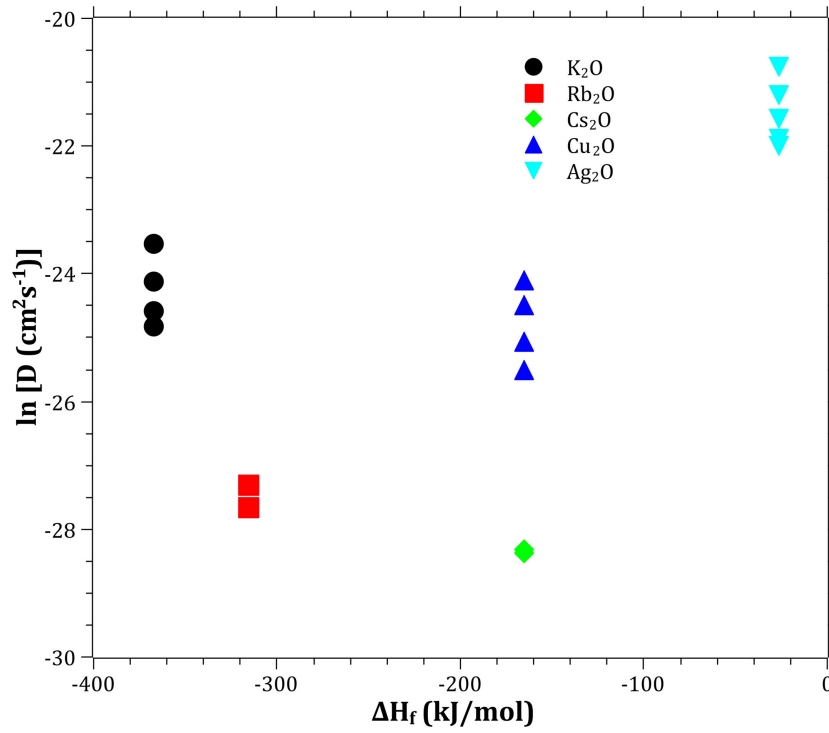


FIGURE 6 | Logarithm of the effective diffusion coefficient vs. enthalpy of formation. Data taken from Dean (1999).

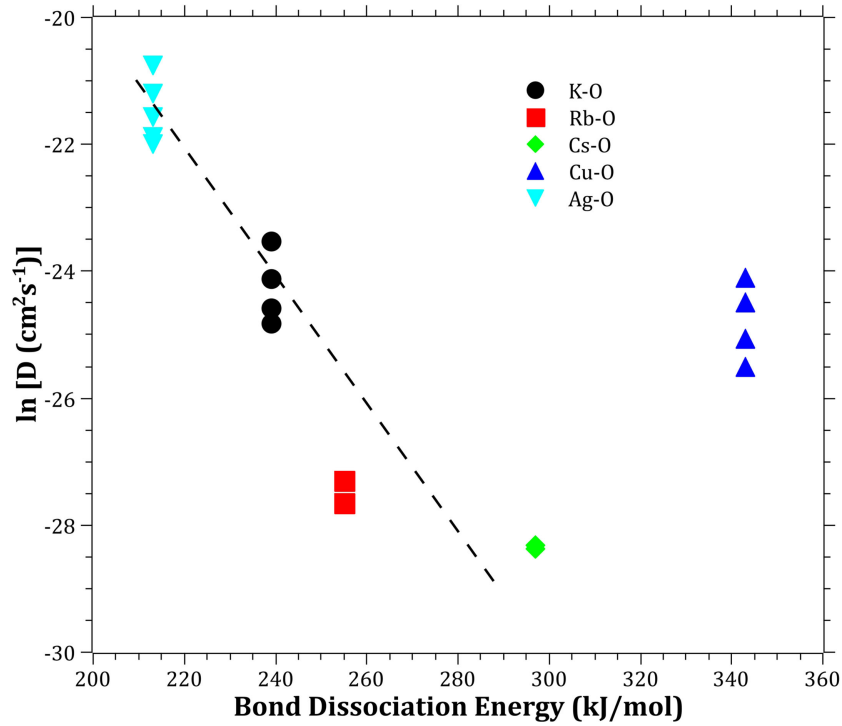
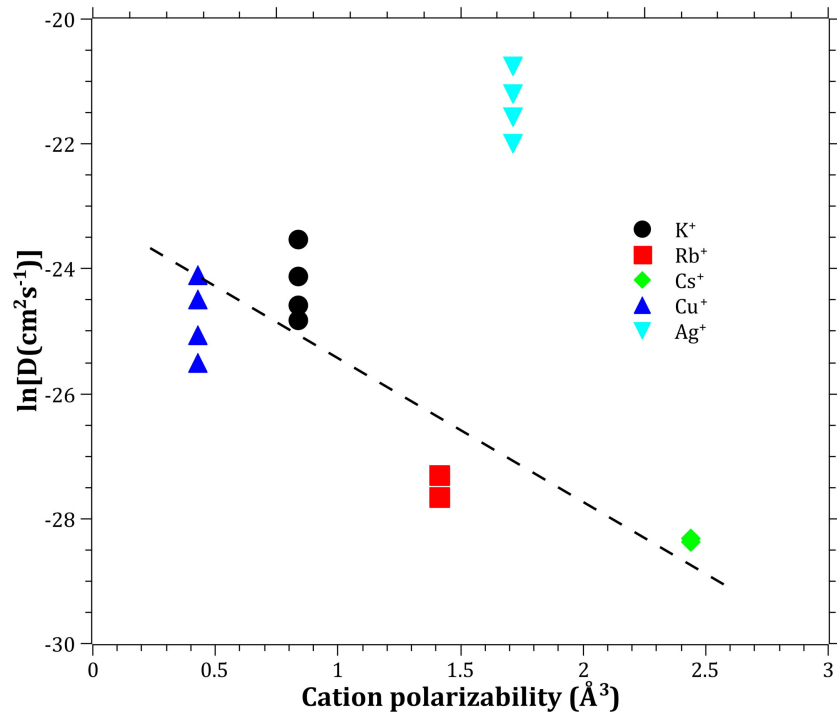
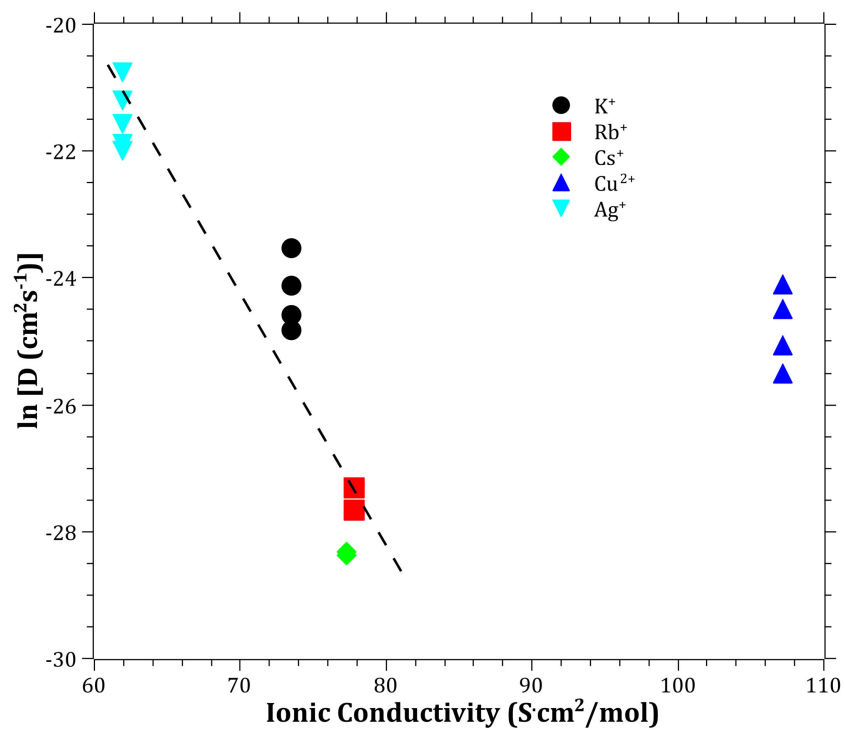


FIGURE 7 | Logarithm of the effective diffusion coefficient vs. bond dissociation energy. Data taken from Dean (1999). The dashed line is a guide to the eye.



**FIGURE 8 |** Logarithm of the effective diffusion coefficient vs. electronic cation polarizability. Molar refraction data taken from Pauling (1927). The dashed line is a guide to the eye.



**FIGURE 9 |** Logarithm of the effective diffusion coefficient vs. aqueous ionic conductivity. Data taken from Dean (1999). The dashed line is a guide to the eye.



considered: (i) large enough structural transport channels (c.f. **Figure 1**), (ii) disordered mobile ion sub-lattice, (iii) highly polarizable mobile ions and anion sub-lattices, and (iv) size of the ions in the vitreous network. The effective diffusion coefficients will always be a complex trade-off between different properties; however, in the current paper, we have found a correlation using bond dissociation energy and electronic cation polarizability. The unusually high effective diffusion coefficient of  $\text{Ag}^+$  as compared to  $\text{Cu}^+$  can at least partly be explained by  $\text{Ag}^+$  having a comparable bond dissociation energy and a high cation polarizability, while  $\text{Cu}^+$  have a high bond dissociation energy and a comparable cation polarizability. This indicates that the breakage of bonds and structural deformability are keys to improving the ion-exchange rate. By identifying the key properties, it will give the possibility for modeling the diffusion by topological, atomistic, or quantum mechanics modeling (Mauro et al., 2016). One should bear in mind that the mobile cations are only one component in the creations of bonds and polarizability in the vitreous network. The anions, most often consisting of oxygen, can also be exchanged for other anions (Wondraczek et al., 2011), such as nitrogen (Becher et al., 2011; Ali et al., 2015) or carbon (Renlund et al., 1991). The understanding that the bond dissociation energy and the polarizability can be correlated to the effective diffusion coefficient also provides a perspective how ionic diffusion and ion-exchange strengthening behave in different types of glasses, including, e.g., chalcogenide or chalcohalide glasses (Calvez et al., 2009). Furthermore, it provides the insight that the alkali ions bond less strongly when charge compensating  $\text{Al}^{3+}$ ,  $\text{B}^{3+}$ , or  $\text{P}^{5+}$  than when creating NBO, i.e., likely a significant difference in the type of bonding, in accordance with (Smedskjaer et al., 2011).

## REFERENCES

- Ali, S., Jonson, B., Pomeroy, M. J., and Hampshire, S. (2015). Issues associated with the development of transparent oxynitride glasses. *Ceram. Int.* 41(3, Part A), 3345–3354. doi:10.1016/j.ceramint.2014.11.030
- Anderson, O. L., and Stuart, D. A. (1954). Calculation of activation energy of ionic conductivity in silica glasses by classical methods. *J. Am. Ceram. Soc.* 37, 573–580. doi:10.1111/j.1151-2916.1954.tb13991.x
- Arletti, R., Dalconi, M. C., Quartieri, S., Triscari, M., and Vezzalini, G. (2006). Roman coloured and opaque glass: a chemical and spectroscopic study. *Appl. Phys. A* 83, 239–245. doi:10.1007/s00339-006-3515-2
- Bartholomew, R. F., and Garfinkel, H. M. (1980). "Chemical strengthening of glass." in *Glass Science and Technology Vol 5 Elasticity and Strength in Glasses*, eds D. R. Uhlmann and N. J. Kreidl (New York: Academic Press), 217–270.
- Becher, P. F., Hampshire, S., Pomeroy, M. J., Hoffmann, M. J., Lance, M. J., and Satet, R. L. (2011). An overview of the structure and properties of silicon-based oxynitride glasses. *Int. J. Appl. Glass Sci.* 2, 63–83. doi:10.1111/j.2041-1294.2011.00042.x
- Bernasconi, A., Dapiaggi, M., Pavese, A., Bowron, D. T., and Imberti, S. (2012). Local structure of Si-Al-Ca-Na-O glasses from coupled neutron and X-ray total scattering data. *J. Phys. Chem. B* 116, 13114–13123. doi:10.1021/jp306697w
- Bunde, A., Funke, K., and Ingram, M. D. (1996). A unified site relaxation model for ion mobility in glassy materials. *Solid State Ionics.* 86–88(Part 2), 1311–1317. doi:10.1016/0167-2738(96)00307-4
- Burggraaf, A. J. (1966). The strengthening of glass by ion exchange part 2: stress formation and stress relaxation after ion exchange in alkali aluminosilicate glasses in connection with structural changes in the glass. *Phys. Chem. Glasses* 7, 166–177.

## CONCLUDING REMARKS

The effective diffusivities of the studied monovalent cations follow the order  $\text{Ag}^+ > \text{K}^+ > \text{Cu}^+ > \text{Rb}^+ > \text{Cs}^+$ . This is in accordance with the order of ionic radii for the alkali ions ( $\text{K}^+ < \text{Rb}^+ < \text{Cs}^+$ ). However, an opposite pattern is found for the noble metal ions, where the ionic radii  $\text{Cu}^+ < \text{Ag}^+$ . The  $\text{Cu}^+$  cation behaves with respect to its small ionic radius peculiar compared to the other ions. The bond dissociation energy offers the best explanation as to why  $\text{Cu}^+$  is slower than  $\text{Ag}^+$ . The polarizability of ions adds another dimension by offering increased structural deformability, which can be a route to enhance the ionic transport. A better understanding of ionic diffusion in glass can give rise to stronger and less expensive chemically strengthened glasses, using adapted combinations of diffusing species. Correlations between bond dissociation energies and polarizability provide an understanding of how different anions in glass affect effective diffusion coefficients and how ionic diffusion in different types of glasses may be tailored.

## AUTHOR CONTRIBUTIONS

SK and LW perceived the idea of the paper. SK wrote the draft of the manuscript. All authors were involved in the discussions and elaborating the manuscript text.

## FUNDING

Funding from Vinnova (Grant No. 2013-04343 for SK and 2015-04809 for SA) co-funded by Marie Curie Actions FP7-PEOPLE-2011-COFUND (GROWTH 291795) is greatly acknowledged.

- Burggraaf, A. J., and Cornelissen, J. (1964). The strengthening of glass by ion exchange part 1: stress formation by ion diffusion in alkali aluminosilicate glass. *Phys. Chem. Glasses* 5, 123–129.
- Calvez, L., Rozé, M., Ma, H. L., Sangleboeuf, J. C., Guin, J.-P., and Zhang, X. H. (2009). Strengthening of chalcogenide glasses by ion exchange. *J. Non Oxide Glasses* 1, 30–37.
- Cao, C., Li, Z.-B., Wang, X.-L., Zhao, X.-B., and Han, W.-Q. (2014). Recent advances in inorganic solid electrolytes for lithium batteries. *Front. Energy Res.* 2:25. doi:10.3389/fenrg.2014.00025
- Cormack, A. N., and Du, J. (2001). Molecular dynamics simulations of soda-lime-silicate glasses. *J. Non Cryst. Solids* 293–295, 283–289. doi:10.1016/S0022-3093(01)00831-6
- Cormier, L., Calas, G., and Cuello, G. J. (2010). Structural study of Ca-Mg and K-Mg mixing in silicate glasses by neutron diffraction. *J. Non Cryst. Solids* 356, 2327–2331. doi:10.1016/j.jnoncrysol.2010.02.023
- Crank, J. (1975). *The Mathematics of Diffusion*. Oxford: Oxford University Press.
- d'Acapito, F., Colonna, S., Mobilio, S., Gonella, F., Cattaruzza, E., and Mazzoldi, P. (1997). Local atomic environment of Cu ions in ion-exchanged silicate glass waveguides: an x-ray absorption spectroscopy study. *Appl. Phys. Lett.* 71, 2611–2613. doi:10.1063/1.120156
- Dean, J. A. (1999). *Lange's Handbook of Chemistry*. McGraw-Hill, Inc.
- Dietzel, A. (1942). Die Kationenfeldstärken und ihre Beziehungen zu Entglasungsvorgängen, zur Verbindungsbildung und zu den Schmelzpunkten von Silicaten. *Z. Elektrochem. Angew. Phys. Chem.* 48, 9–23. doi:10.1002/bbpc.19420480104
- Doremus, R. H. (1964). Exchange and diffusion of ions in glass. *J. Phys. Chem.* 68, 2212. doi:10.1021/j100790a031

- Du, J., and Cormack, A. N. (2004). The medium range structure of sodium silicate glasses: a molecular dynamics simulation. *J. Non Cryst. Solids* 349, 66–79. doi:10.1016/j.jnoncrysol.2004.08.264
- Dubiel, M., Brunsch, S., Kolb, U., Gutwerk, D., and Bertagnolli, H. (1997). Experimental studies investigating the structure of soda-lime glasses after silver-sodium ion exchange. *J. Non Cryst. Solids* 220, 30–44. doi:10.1016/S0022-3093(97)00230-5
- Farges, F., Etcheverry, M.-P., Scheidegger, A., and Grolimund, D. (2006). Speciation and weathering of copper in “copper red ruby” medieval flashed glasses from the Tours cathedral (XIII century). *Appl. Geochem.* 21, 1715–1731. doi:10.1016/j.apgeochem.2006.07.008
- Frischat, G. H. (1975). *Ionic Diffusion in Oxide Glasses*. Aedermannsdorf: Trans Tech Publications.
- Frischat, G. H., Poggemann, J. F., and Heide, G. (2004). Nanostructure and atomic structure of glass seen by atomic force microscopy. *J. Non Cryst. Solids* 345–346, 197–202. doi:10.1016/j.jnoncrysol.2004.08.022
- George, A. M., and Stebbins, J. F. (1996). Dynamics of Na in sodium aluminosilicate glasses and liquids. *Phys. Chem. Miner.* 23, 526–534. doi:10.1007/bf00242002
- Gliozzo, E., Santagostino Barbone, A., D’Acapito, F., Turchiano, M., Turbanti Memmi, I., and Volpe, G. (2010). The sectilia panels of Faragola (Ascoli Satriano, Southern Italy): a multi-analytical study of the green, marbled (green and yellow), blue and blackish glass slabs. *Archaeometry* 52, 389–415. doi:10.1111/j.1475-4754.2009.00493.x
- Gonella, F., Caccavale, F., Bogomolova, L. D., D’Acapito, F., and Quaranta, A. (1998). Experimental study of copper-alkali ion exchange in glass. *J. Appl. Phys.* 83, 1200–1206. doi:10.1063/1.366816
- Gonella, F., Quaranta, A., Padovani, S., Sada, C., D’Acapito, F., Maurizio, C., et al. (2005). Copper diffusion in ion-exchanged soda-lime glass. *Appl. Phys. A Mater. Sci. Process.* 81, 1065–1071. doi:10.1007/s00339-004-2949-7
- Grandjean, A., Malki, M., Simonnet, C., Manara, D., and Penelon, B. (2007). Correlation between electrical conductivity, viscosity, and structure in borosilicate glass-forming melts. *Phys. Rev. B* 75, 054112. doi:10.1103/PhysRevB.75.054112
- Greaves, G. (1981). Sodium environments in glass. *J. Phys. Colloq.* 42, C4–C225. doi:10.1051/jphyscol:1981447
- Greaves, G. N. (1985). EXAFS and the structure of glass. *J. Non Cryst. Solids* 71, 203–217. doi:10.1016/0022-3093(85)90289-3
- Greaves, G. N., Fontaine, A., Lagarde, P., Raoux, D., and Gurman, S. J. (1981). Local structure of silicate glasses. *Nature* 293, 611–616. doi:10.1038/293611a0
- Greaves, G. N., Gurman, S. J., Catlow, C. R. A., Chadwick, A. V., Houde-Walter, S., Henderson, C. M. B., et al. (1991). A structural basis for ionic diffusion in oxide glasses. *Philos. Mag.* A 64, 1059–1072. doi:10.1080/01418619108204878
- Griebenow, K., Hoppe, U., Mönck, D., Kamitsos, E. I., and Wondraczek, L. (2017). Transition-metal incorporation and Co-Sr/Mn-Sr mixed-modifier effect in metaphosphate glasses. *J. Non Cryst. Solids* 460, 136–145. doi:10.1016/j.jnoncrysol.2017.01.022
- Gy, R. (2003). Stress corrosion of silicate glass: a review. *J. Non Cryst. Solids* 316, 1–11. doi:10.1016/S0022-3093(02)01931-2
- Honkanen, S., West, B. R., Yliniemi, S., Madasamy, P., Morrell, M., Auxier, J., et al. (2006). Recent advances in ion exchanged glass waveguides and devices. *Phys. Chem. Glasses* 47, 110–120.
- Houde-Walter, S. N., Inman, J. M., Dent, A. J., and Greaves, G. N. (1993). Sodium and silver environments and ion-exchange processes in silicate and aluminosilicate glasses. *J. Phys. Chem.* 97, 9330. doi:10.1021/j100139a013
- Jackson, W. E., Brown, G. E., and Ponader, C. W. (1987). X-ray absorption study of the potassium coordination environment in glasses from the NaAlSi3O8-KAlSi3O8 binary. *J. Non Cryst. Solids* 93, 311–322. doi:10.1016/S0022-3093(87)80177-1
- Kamijo, N., Handa, K., and Umesaki, N. (1996). Soft X-ray XAFS studies on the local structure of K2O-SiO2 glasses. *JIM Mater. Trans.* 37, 927–931. doi:10.2320/matertrans1989.37.927
- Kamiya, K., Okasaka, K., Wada, M., Nasu, H., and Yoko, T. (1992). Extended X-ray absorption fine structure (EXAFS) study on the local environment around copper in low thermal expansion copper aluminosilicate glasses. *J. Am. Ceram. Soc.* 75, 477–478. doi:10.1111/j.1151-2916.1992.tb08205.x
- Karlsson, S. (2012). *Doctoral Thesis: Modification of Float Glass Surfaces by Ion Exchange*. Ph.D., Linnaeus University.
- Karlsson, S., Ali, S., Limbach, R., Strand, M., and Wondraczek, L. (2015). Alkali salt vapour deposition and in-line ion exchange on flat glass surfaces. *Glass Technol. Eur. J. Glass Sci. Technol. A* 56, 203–213. doi:10.13036/1753-3546.56.6.203
- Karlsson, S., Grund Bäck, L., Kidkhunthod, P., Lundstedt, K., and Wondraczek, L. (2016). Effect of TiO2 on optical properties of glasses in the soda-lime-silicate system. *Opt. Mater. Expr.* 6, 1198–1216. doi:10.1364/ome.6.001198
- Karlsson, S., Jonson, B., Reibstein, S., and Wondraczek, L. (2013). Surface ruby colouring of float glass by sodium – copper ion exchange. *Eur. J. Glass Sci. Technol. A Glass Technol.* 54, 100–107.
- Karlsson, S., Jonson, B., and Stålhandske, C. (2010a). The technology of chemical glass strengthening – a review. *Eur. J. Glass Sci. Technol. A Glass Technol.* 51, 41–54.
- Karlsson, S., Jonson, B., Sundberg, P., and Stålhandske, C. (2010b). Surface analysis of float glass using surface ablation cell (SAC) part 2: determination of the diffusion characteristics of K<sup>+</sup>-Na<sup>+</sup> Ion exchange. *Eur. J. Glass Sci. Technol. A Glass Technol.* 51, 55–62.
- Karlsson, S., Jonson, B., and Wondraczek, L. (2012). Copper, silver, rubidium and caesium ion exchange in soda-lime-silicate float glass by direct deposition and in line melting of salt pastes. *Eur. J. Glass Sci. Technol. A Glass Technol.* 53, 1–7.
- Klysubun, W., Thongkam, Y., Pongkrapan, S., Won-in, K., T-Thienprasert, J., and Dararutana, P. (2011). XAS study on copper red in ancient glass beads from Thailand. *Anal. Bioanal. Chem.* 399, 3033–3040. doi:10.1007/s00216-010-4219-1
- Kreski, P. K., Varshneya, A. K., and Cormack, A. N. (2012). Investigation of ion-exchange ‘stuffed’ glass structures by molecular dynamics simulation. *J. Non Cryst. Solids* 358, 3539–3545. doi:10.1016/j.jnoncrysol.2012.05.025
- Lee, J., Yano, T., Shibata, S., Nukui, A., and Yamane, M. (2000). EXAFS study on the local environment of Cu<sup>+</sup> ions in glasses of the Cu2O–Na2O–Al2O3–SiO2 system prepared by Cu<sup>+</sup>/Na<sup>+</sup> ion exchange. *J. Non Cryst. Solids* 277, 155–161. doi:10.1016/S0022-3093(00)00330-6
- Liu, K., and Pun, E. Y. B. (2004). Single-mode Rb<sup>+</sup>-K<sup>+</sup> ion-exchanged BK7 glass waveguides with low losses at 1550 nm. *IEEE Photonics Technol. Lett.* 16, 120–122. doi:10.1109/LPT.2003.818921
- Maass, P., Bunde, A., and Ingram, M. D. (1992). Ion transport anomalies in glasses. *Phys. Rev. Lett.* 68, 3064–3067. doi:10.1103/PhysRevLett.68.3064
- Martin, S. W., and Angell, C. A. (1986). Dc and ac conductivity in wide composition range Li2O-P2O5 glasses. *J. Non Cryst. Solids* 83, 185–207. doi:10.1016/0022-3093(86)90067-0
- Mauro, J. C., Tandia, A., Vargheese, K. D., Mauro, Y. Z., and Smedskjaer, M. M. (2016). Accelerating the design of functional glasses through modeling. *Chem. Mater.* 28, 4267–4277. doi:10.1021/acs.chemmater.6b01054
- McKeown, D. A., Waychunas, G. A., and Brown, G. E. (1985). Exafs and xanes study of the local coordination environment of sodium in a series of silica-rich glasses and selected minerals within the Na2O•Al2O3•SiO2 system. *J. Non Cryst. Solids* 74, 325–348. doi:10.1016/0022-3093(85)90078-X
- Morozumi, H., Nakano, H., Yoshida, S., and Matsuoka, J. (2015). Crack initiation tendency of chemically strengthened glasses. *Int. J. Appl. Glass Sci.* 6, 64–71. doi:10.1111/ijag.12089
- Nordberg, M. E., Mochel, E. L., Garfinkel, H. M., and Olcott, J. S. (1964). Strengthening by ion exchange. *J. Am. Ceram. Soc.* 47, 215–219. doi:10.1111/j.1151-2916.1964.tb14399.x
- Opilski, A., Rogoziński, R., Gut, K., Błachut, M., and Opilski, Z. (2000). Present state and perspectives involving application of ion exchange in glass. *Opto-Electron. Rev.* 8, 117–127.
- Pask, J. A., and Parmelee, C. W. (1943). Study of diffusion in glass. *J. Am. Ceram. Soc.* 26, 267. doi:10.1111/j.1151-2916.1943.tb15214.x
- Pauling, L. (1927). The theoretical prediction of the physical properties of many-electron atoms and ions. Mole refraction, diamagnetic susceptibility, and extension in space. *Proc. R. Soc. Lond. Ser. A Containing Pap. Math. Phys. Character* 114, 181–211. doi:10.1098/rspa.1927.0035
- Poletto Rodrigues, B., Deubener, J., and Wondraczek, L. (2016). Modifier interaction and mixed-alkali effect in bond constraint theory applied to ternary alkali metaphosphate glasses. *Front. Mater.* 3:25. doi:10.3389/fmats.2016.00025
- Ragoen, C., Sen, S., Lambricht, T., and Godet, S. (2017). Effect of Al2O3 content on the mechanical and interdiffusional properties of ion-exchanged

- Na-aluminosilicate glasses. *J. Non Cryst. Solids* 458, 129–136. doi:10.1016/j.jnoncrysol.2016.12.019
- Ramaswamy, R. V., and Srivastava, R. (1988). Ion-exchanged glass waveguides: a review. *J. Lightwave Technol.* 6, 984. doi:10.1109/50.4090
- Ravaine, D., and Souquet, J. (1977). Thermodynamic approach to ionic conductivity in oxide glasses; I, correlation of the ionic conductivity with the chemical potential of alkali oxide in oxide glasses. *Phys. Chem. Glasses* 18, 27–31.
- Renlund, G. M., Prochazka, S., and Doremus, R. H. (1991). Silicon oxycarbide glasses: part II. Structure and properties. *J. Mater. Res.* 6, 2723–2734. doi:10.1557/JMR.1991.2723
- Schaeffer, H. A. (2012). Transport phenomena and diffusion anomalies in glass. *Mater. Ceram.* 64, 156–161.
- Schulze, G. (1913). Versuche über die diffusion von silber in glas. *Ann. Phys.* 345, 335–367. doi:10.1002/andp.19133450208
- Shaisha, E. E., and Cooper, A. R. (1981). Ion exchange of soda-lime glass with univalent cations. *J. Am. Ceram. Soc.* 64, 278–283. doi:10.1111/j.1151-2916.1981.tb09602.x
- Shannon, R. (1976). Revised effective ionic radii and systematic studies of interatomic distances in halides and chalcogenides. *Acta Crystallogr. A Cryst. Phys. Diffraction. Gen. Crystallogr.* 32, 751–767. doi:10.1107/S0567739476001551
- Smedskjaer, M. M., Zheng, Q., Mauro, J. C., Potuzak, M., Mörup, S., and Yue, Y. (2011). Sodium diffusion in boroaluminosilicate glasses. *J. Non Cryst. Solids* 357, 3744–3750. doi:10.1016/j.jnoncrysol.2011.07.008
- Stefanovsky, S. V., and Purans, J. J. (2012). Cesium speciation in nuclear waste glasses. *Phys. Chem. Glasses* 53, 186–190.
- Stern, K. H. (1966). Glass-molten salt interactions. *Chem. Rev.* 66, 355. doi:10.1021/cr60242a001
- Sundberg, P., Karlsson, S., Brochot, D., Strubel, C., and Simons, J. (2010). Surface analysis of float glass using surface ablation cell (SAC) part 1: initial collaboration and comparison with SIMS. *Eur. J. Glass Sci. Technol. A Glass Technol.* 51, 13–21.
- Tervonen, A., West, B. R., and Honkanen, S. (2011). Ion-exchanged glass waveguide technology: a review. *Opt. Eng.* 50, 071107. doi:10.1117/1.3559213
- Uhlig, H., Hoffmann, M. J., Lamparter, H.-P., Aldinger, F., Bellissent, R., and Steeb, S. (1996). Short-Range and medium-range order in lithium silicate glasses, part I: diffraction experiments and results. *J. Am. Ceram. Soc.* 79, 2833–2838. doi:10.1111/j.1151-2916.1996.tb08716.x
- Varshneya, A. K. (2006). *Fundamentals of Inorganic Glasses*. Sheffield, UK: Society of Glass Technology.
- Varshneya, A. K. (2010a). Chemical strengthening of glass: lessons learned and yet to be learned. *Int. J. Appl. Glass Sci.* 1, 131–142. doi:10.1111/j.2041-1294.2010.00010.x
- Varshneya, A. K. (2010b). The physics of chemical strengthening of glass: room for a new view. *J. Non Cryst. Solids* 356, 2289–2294. doi:10.1016/j.jnoncrysol.2010.05.010
- Vessal, B., Greaves, G. N., Marten, P. T., Chadwick, A. V., Mole, R., and Houde-Walter, S. (1992). Cation microsegregation and ionic mobility in mixed alkali glasses. *Nature* 356, 504–506. doi:10.1038/356504a0
- Vogel, W. (1994). *Glass Chemistry*. Berlin: Springer Science+Business Media.
- Weigel, C., Cormier, L., Calas, G., Galoisy, L., and Bowron, D. T. (2008). Nature and distribution of iron sites in a sodium silicate glass investigated by neutron diffraction and EPSR simulation. *J. Non Cryst. Solids* 354, 5378–5385. doi:10.1016/j.jnoncrysol.2008.09.030
- Wondraczek, L., Mauro, J. C., Eckert, J., Kühn, U., Horbach, J., Deubener, J., et al. (2011). Towards ultrastrong glasses. *Adv. Mater. Weinheim* 23, 4578–4586. doi:10.1002/adma.201102795
- Xu, Z., and Stebbins, J. F. (1995). 6Li nuclear magnetic resonance chemical shifts, coordination number and relaxation in crystalline and glassy silicates. *Solid State Nucl. Magn. Reson.* 5, 103–112. doi:10.1016/0926-2040(95)00026-M
- Yang, X. C., and Dubiel, M. (2007). XAFS studies of silver environments in ion-exchanged glasses. *AIP Conf. Proc.* 882, 457–459. doi:10.1063/1.2644557
- Yang, X. C., Dubiel, M., Brunsch, S., and Hofmeister, H. (2003). X-ray absorption spectroscopy analysis of formation and structure of Ag nanoparticles in soda-lime silicate glass. *J. Non Cryst. Solids* 328, 123–136. doi:10.1016/S0022-3093(03)00469-1
- Zeng, H., Wang, L., Ye, F., Yang, B., Chen, J., Chen, G., et al. (2016). Mechanical-structural investigation of chemical strengthening aluminosilicate glass through introducing phosphorus pentoxide. *Front. Mater.* 3:53. doi:10.3389/fmats.2016.00053
- Zhao, J., Gaskell, P. H., Cluckie, M. M., and Soper, A. K. (1998). A neutron diffraction, isotopic substitution study of the structure of Li<sub>2</sub>O-2SiO<sub>2</sub> glass. *J. Non Cryst. Solids* 232–234, 721–727. doi:10.1016/S0022-3093(98)00554-7

**Conflict of Interest Statement:** The authors declare that the research was conducted in the absence of any commercial or financial relationships that could be construed as a potential conflict of interest.

Copyright © 2017 Karlsson, Wondraczek, Ali and Jonson. This is an open-access article distributed under the terms of the Creative Commons Attribution License (CC BY). The use, distribution or reproduction in other forums is permitted, provided the original author(s) or licensor are credited and that the original publication in this journal is cited, in accordance with accepted academic practice. No use, distribution or reproduction is permitted which does not comply with these terms.